Journal of Molecular Structure 1250 (2022) 131717

Contents lists available at ScienceDirect

Journal of Molecular Structure

journal homepage: www.elsevier.com/locate/molstr

Tautomerism and IR spectroscopy of arylsulfonamides by quantum mechanical calculations

Francisco-Márquez Misaela[a], Pérez de la Luz Alexander[b,c], Soriano-Correa Catalina[d,*], Barrientos-Salcedo Carolina[d,e], Sainz-Díaz C. Ignacio[c,*]

[a] Instituto Politécnico Nacional-UPIICSA, Té 950, Col. Granjas Mexico, C.P. 08400 Mexico City, Mexico
[b] Departamento de Química, Universidad Autónoma Metropolitana-Iztapalapa. Av. San Rafael Atlixco 186, Col. Vicentina, Mexico City, 09340, Mexico
[c] Instituto Andaluz de Ciencias de la Tierra, Consejo Superior de Investigaciones Científicas-Universidad de Granada, Av. de las Palmeras, 4, 18100-Armilla, Granada, Spain
[d] Unidad de Química Computacional, Facultad de Estudios Superiores Zaragoza, Universidad Nacional Autónoma de México, Iztapalapa, C.P. 09230 Mexico City, Mexico
[e] Laboratorio de Química Médica y Quimiogenómica, Facultad de Bioanálisis Campus Veracruz, Universidad Veracruzana, C.P. 91700, Veracruz, Mexico

ARTICLE INFO

Article history:
Received 31 August 2021
Revised 5 October 2021
Accepted 11 October 2021
Available online 20 October 2021

Keywords:
Sulfonamides
Tautomerism
IR spectroscopy
Crystal polymorphism
Quantum mechanical calculations

ABSTRACT

The molecular structures of sulphonamides are interesting for evaluating their mobility in soils and preparing composite complexes for optimizing the use of these drugs. In this work, the molecular structures of several arylsulfonamides along with conformational analysis and tautomerism were investigated theoretically. The spectroscopical properties of several arylsulfonamides, were also studied at molecular level by using a computational modeling at quantum mechanics level. Besides, the controversial experimental results found in the infrared (IR) spectroscopy bands assignments of solid sulphonamides pushed us up to study computationally the crystal structure of sulfamethazine for clarifying previous assignment discrepancies. The previously proposed polymorphism in the crystal structure of this drug has been also clarified in this work.

1. Introduction

Almost a century after the discovery of the antibacterial activity of sulfanilamide, many N1- substituted sulfonamides have been extensively tested due to their bacteriostatic activity against human and veterinary pathogens [1–3]. Owing to their relatively low-cost and high efficiency against many bacterial infections, sulfonamides are one of the most used groups of antibiotics employed in the veterinary and human medical sectors, and consequently are widely found in natural waters [4] and, soils [5]. Consequently, an important worldwide environmental problem is reaching derived from the intensive use of pharmaceutical drugs for humans and animals, especially in farming and livestock industry, which leads to pharmaco-pollution.

The bacteriostatic activity of the arylsulfonamides is their biomimetism with the p-aminobenzoic acid in the folic acid metabolism path. In addition to their antimicrobial use, the arylsulfonamides have also many therapeutic applications as antifungal, antidiabetic, antiglaucoma, antiallergic, antiobesic, vasodilator, anti-HIV, and anticancer [6].

The sulfonamides belong to an antibiotic class extensively used in animal and human treatment, which explains their presence in the aquatic environment; so that, in the last two decades, the sulfamethazine (SMT) and sulfamethoxazole (SMX), sulfachloropyridazine (SCP) and sulfacetamide (SCM) (Fig. 1) drugs are detectable along with their metabolites and present in wastewater and sewage at high concentrations relative to other analyzed antibiotics. They are released in farming land interacting with soil components and can be washed off into raining water, surface water and reached the ground waters. The residues of these drugs can enter to the food chain and impact on environment and affect to the human health. The presence of these pollutants in food samples is a major environmental concern, developing antibiotic resistance to pathogenic bacteria.

Therefore, further studies at molecular level should be developed, with the purpose to know the chemical structure,

* Corresponding authors.
E-mail addresses: csorico@comunidad.unam.mx (S.-C. Catalina), ci.sainz@csic.es (S.C. Ignacio).

https://doi.org/10.1016/j.molstruc.2021.131717

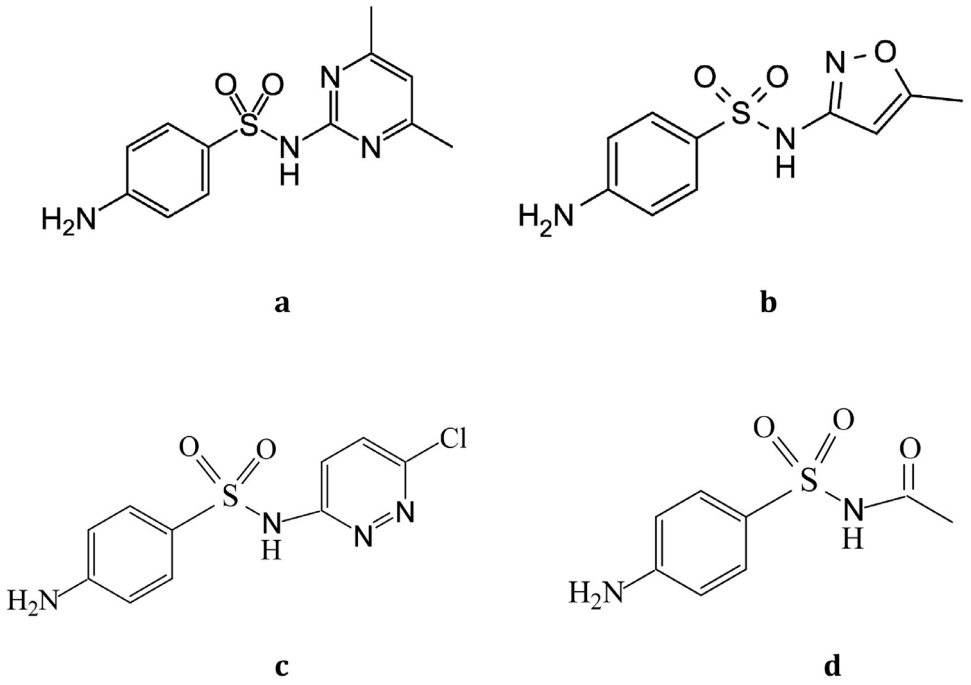

Fig. 1. Sulfonamides molecular structure, a) sulfamethazine, b) Sulfametoxazole, c) sulfachloropyridazine, and d) sulfacetamide.

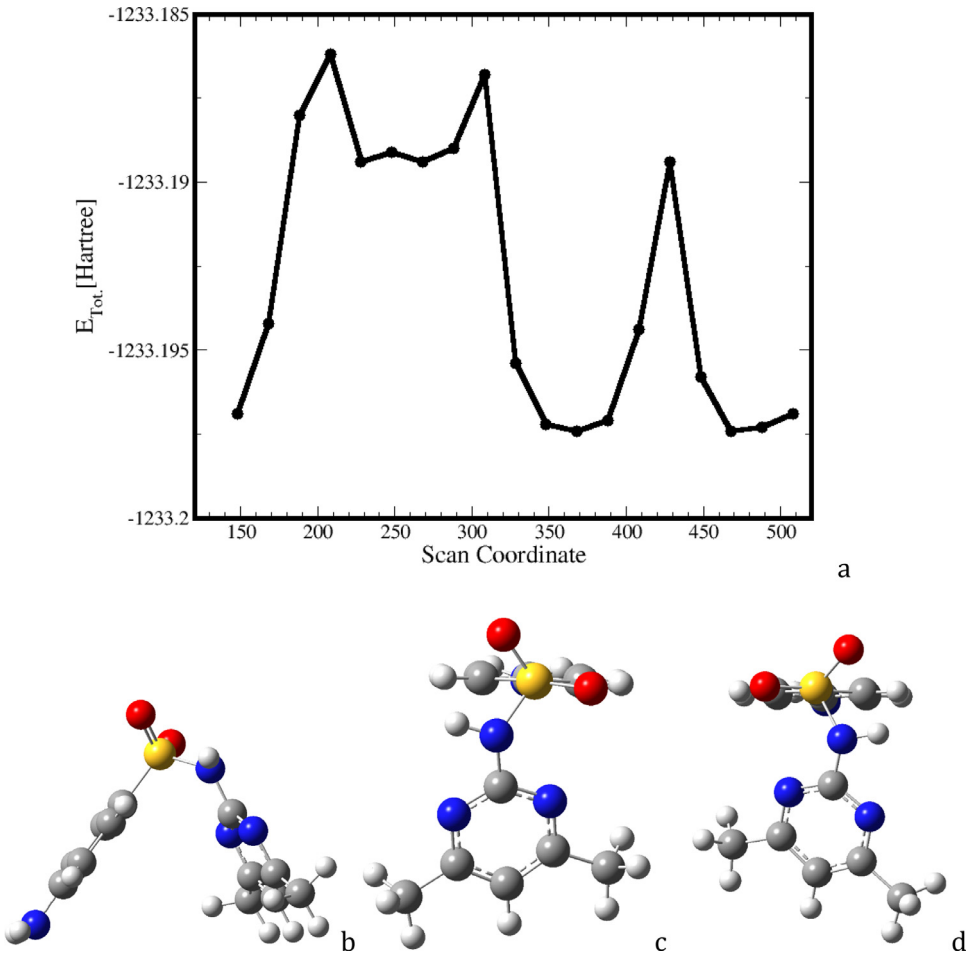

Fig. 2. Scanning of the O-S-N–H dihedral angle of sulfamethazine (a) and the optimized minima SMT-M1 (b), SMT-M1 viewed from the sulfoxide group in a perpendicular plane of the H_2N-S axis (c), and SMT-M2 (d).

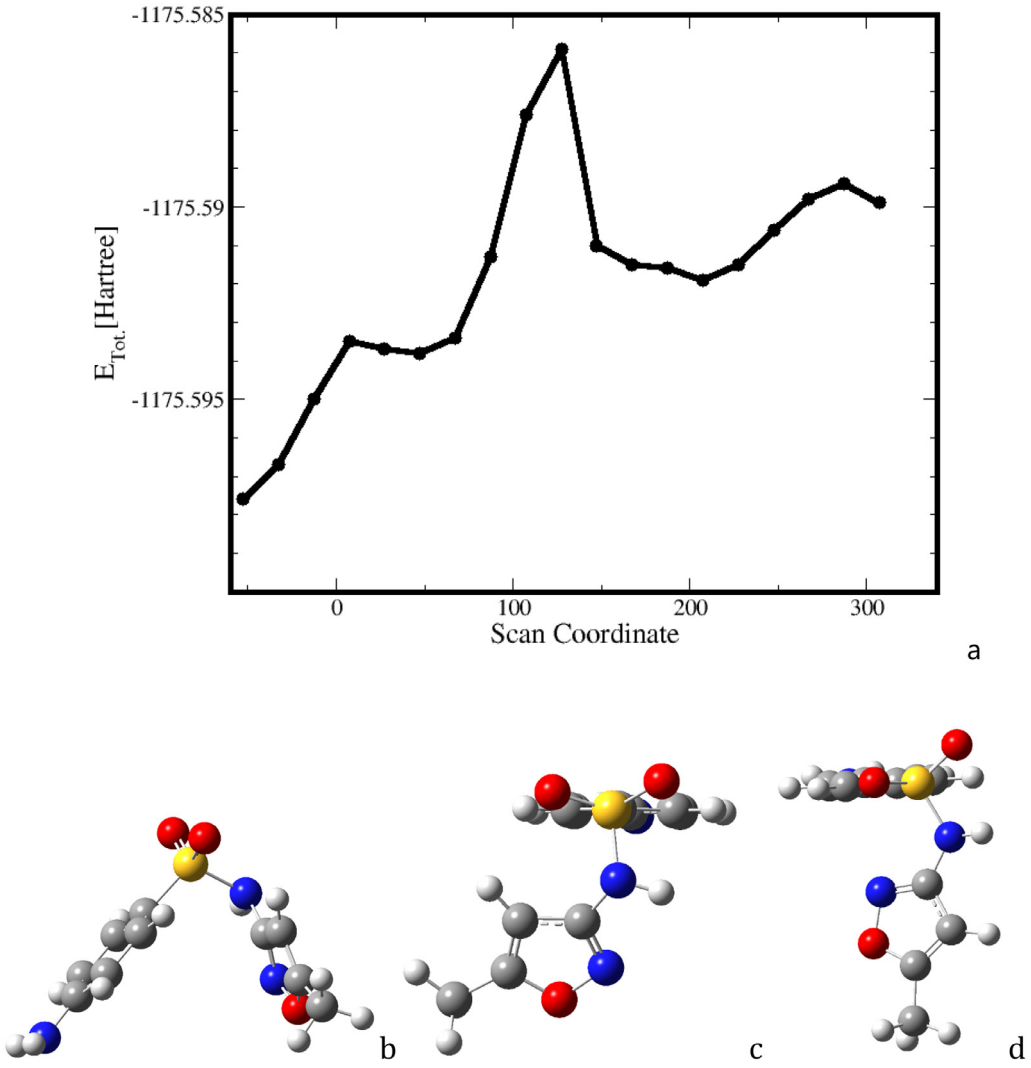

Fig. 3. Scanning of the CCNS dihedral angle of SMX (a), and the optimized minima SMX-M1 (b), SMX-synM1 viewed from the sulfoxide group in a perpendicular plane of the H_2N-S axis (c), and SMX-anti (d).

physicochemical properties, and the intermolecular interactions to reduce the presence of the sulfamides in the aquatic and soils environment.

The great importance of sulfonamides as antibiotic enhanced the research on crystal polymorphism of these drugs in the last decades [7]. However, some authors claimed new crystal forms, which were not actual new polymorphs. Then, there are some discrepancies concerning the number of polymorphs in some sulfonamides.

Molecular calculations have been applied to the study of the molecular and crystal structures [8–10] of drugs describing the intramolecular and intermolecular interactions [11] responsible of the stability of crystal polymorphs [12]. One of the aims of this work is the study of the molecular structure of several arylsulfonamides with different N-substituents in the sulfonamido group at quantum mechanics calculation level. The effect of the nature of these N-substituents on some properties, such as, tautomerism and spectroscopical properties is investigated. Other aim of this work is the exploration of the crystal polymorphism of these arylsulfonamides in order to clarify the discrepancies reported previously in this subject.

2. Models

Sulfamethazine (4-Amino-N-(4,6-dimethyl-2-pyrimidinyl)-benzenesulfonamide) (SMT) [13–15], sulfamethoxazole (4-Amino-N-(5-methyl-3-isoxazolyl)-benzenesulfonamide) (SMX) [15], Sulfachloropyridazine (4-amino-N-(6–chloro-3-pyridazinyl)-benzenesulfnamide) (SCP) [16], and sulfacetamide (p-aminobenzene sulfonacetamide) (SCM) [17] crystal structures were taken from previous experimental crystallographic X-ray diffraction data. The sulfonamide molecules were extracted from their crystal structures.

The selection of these arylsulfonamides is based on comparing different N substituents to explore the effect of these substitutions on their properties. Different heterocycles were explored, such as a symmetric pyrimidine (SMT), a five-atoms heterocyclic ring as isoxazole (SMX), an asymmetric pyridazyl ring (SCP), and with only an acetyl group without heterocyclic moiety (SCM) (Fig. 1).

3. Methodology

Quantum mechanical calculations were applied for the study of molecules, and crystal structures. Isolated molecules were cal-

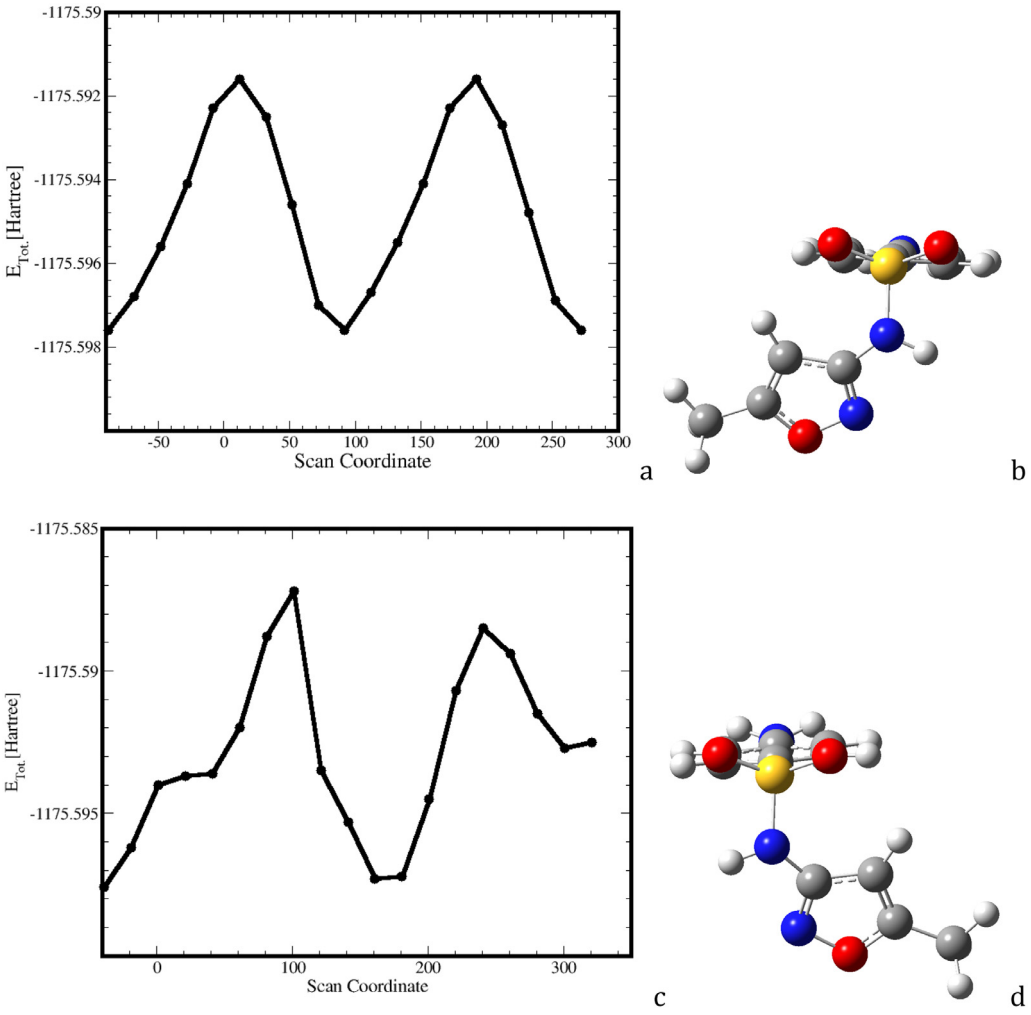

Fig. 4. Scanning of the SMX dihedral angle CCSN (a) with its second minimum SMX-synM2 (b), and scanning of HNSO (c) with its second minimum SMX-synM3 (d).

culated using the Gaussian 09 program suite [18]. The molecular structures of sulfonamides were optimized with the M06–2X functional, a hybrid meta exchange-correlation functional that is a good functional for aromatic groups, and describes well the non-covalent interactions [19,20]. This functional was used with the 6–311+*G*(d,p) basis set [21]. Optimized geometries were characterized by harmonic vibrational frequencies, which confirmed that the structures obtained are minima on the potential energy surface. The energy calculations have been corrected with the zero-point energy. All calculations were undertaken in an aqueous solution; the solvent effect was described by through the SMD model [22]. In tautomerism studies, the transition states (TS) of the reaction paths were localized performing an IRC (Intrinsic Reaction Coordinate) for both directions.

The isolated molecules embedded in periodical boxes of 20×20×20 Å and the crystal structures were calculated with Density Functional Theory (DFT) applying periodical boundary conditions. This computational approach and methodology were proven useful for studying other drugs [23–26]. We used the Quantum-Espresso (QE) [27] code based on plane wave basis sets, with the generalized gradient approximation (GGA), and the Perdew-Burke-Ernzerhof functional (PBE) for the exchange-correlation potential [28]. Plane wave PAW (Projector Augmented Wave) pseudopotentials [29] were used. In addition, different values of energy cutoff E_{cut}(wfc) (40 –120 Ry) and cutoff for the charge density (160 – 840 Ry) were tested to find the optimal calculation conditions (Fig. S1 in Supporting Information). This preliminary study allowed the optimization of the calculation parameters in order to obtain the maximum precision and reliability of the simulation with the minimum computational cost. The energy cutoff E_{cut}(wfc) used was 100 Ry and with a cutoff of 400 Ry for the charge density (Fig. S1). In all calculations dispersion corrections were included according to the DFT-D3 [30] scheme. All calculations were performed in the at the Γ point of the Brillouin zone. The normal modes of vibration of the crystals were obtained from phonon calculations based on the theory of density functional perturbation (DFPT) [31]. The spectroscopical vibration modes were analysed by using the Molden code [32] The powder X-ray diffraction patterns were simulated from the crystal structures by using the REFLEX code [33].

4. Results and discussion

4.1. Molecular structure

The molecular structures of these antibiotics were optimized as isolated molecules, observing that in both molecules the aromatic and heterocyclic rings are placed in a quasi co-planar orientation but the central axes of these rings form an angle close to 90° (Fig. 2a). Probably a π-π interaction between both rings is responsible of this orientation. Several conformational analyses were performed scanning several dihedral angles in 20° steps. The sulfamethazine (SMT) molecule is highly symmetric and only a sig-

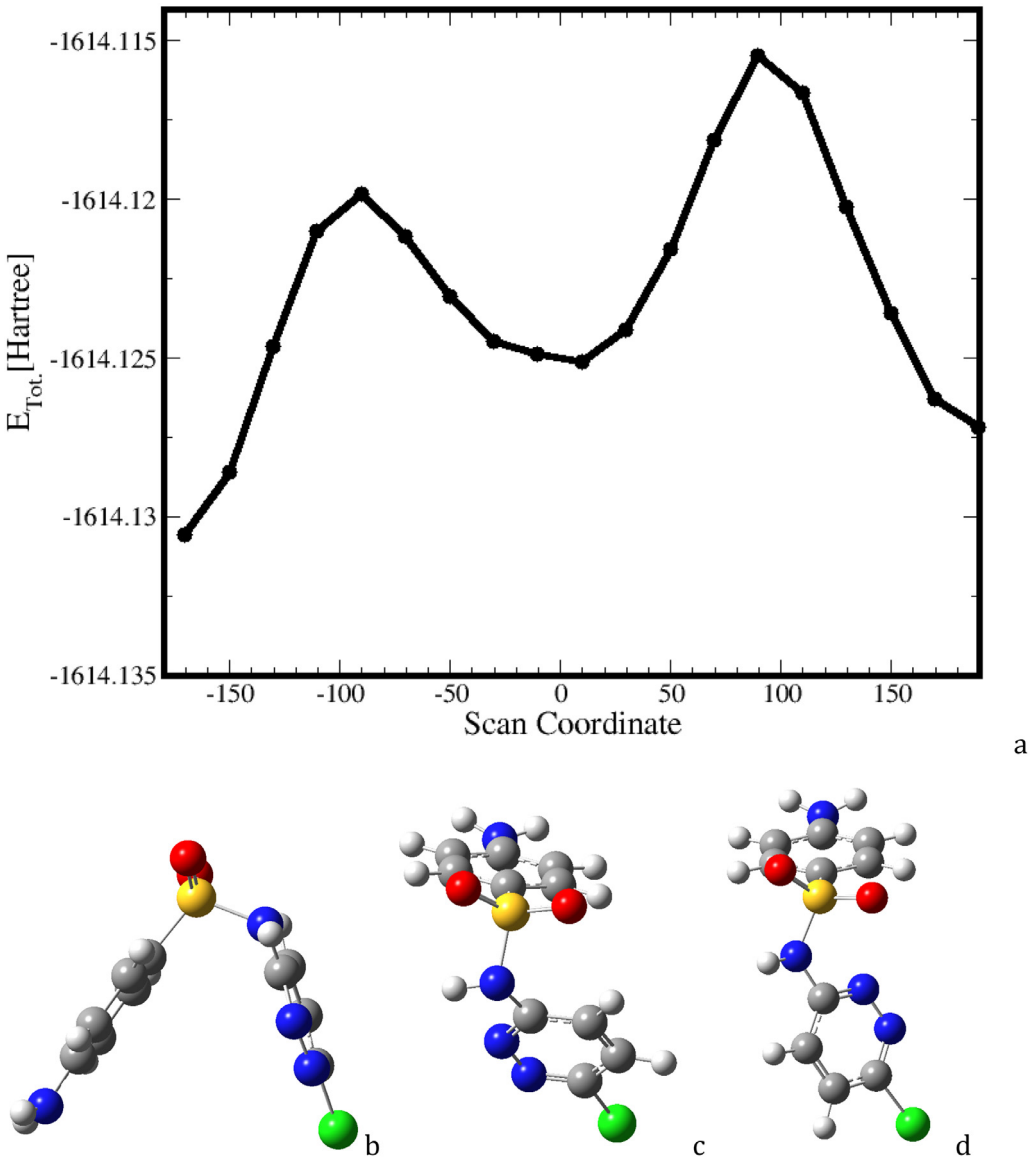

Fig. 5. Scanning of the HNCC dihedral angle of SCP (a), and the optimized minima SCP-M1 (b), SCP-M1 (syn) viewed from the sulfoxide group in a perpendicular plane of the H_2N-S axis (c), and SCP-M2 (anti) (d).

nificant conformation analysis can be performed taking into account the rotation of the heterocyclic ring with respect to the aromatic ring along the dihedral angle O-S-N–H, where the rotor is the S-N bond (Fig. 2a). Some intense sharp peaks are observed in the scanning profile probably because the scan step of 20º is large enough for including several strong changes in the structure forced by steric hindrances. Two main minima are distinguished taking into account the relative orientation of the N–H bond with respect to the aromatic ring observed from the sulfoxide group, SMT-M1 (Fig. 2b, 2c) where the N–H bond is oriented to the left and SMT-M2 (Fig. 2d) with the N–H bond in the right orientation. These minima have similar energy and the most stable is SMT-M2 with only 0.051 kcal/mol of energy difference. Hence, both conformers can exist although their exchange has a barrier close to 6 kcal/mol. The dipole moments of both conformers are similar, SMT-M1 = 13.67 D; SMT-M2= 13.55 D, and the effect of solvent polarity will be negligible.

In the sulfamethoxazole (SMX) molecule several possible conformers can be considered. In the rotation of the CCNS dihedral angle around the C–N bond as a rotor, two minima can be distinguished (Fig. 3a), where the N–H bond can be oriented towards (conformer syn) or against (conformer anti) the heterocyclic N atom (Fig. 3). The conformer syn, SMX-synM1 (Fig. 3b, 3c), is 1.83 kcal/mol more stable than anti (SMX-anti) (Fig. 3d), due probably to the repulsive interactions between the electron clouds of N and sulfoxide O atoms. However, the rotation barrier is small, around 1.44 kcal/mol. Besides, for the rotation of the CCSN dihedral angle, around the C-S bond as a rotor, two minima were detected (Fig. 4a), where the aromatic ring rotates. A sharp peak is showed in these profiles (Fig, 3a and 4c) probably because strong steric hindrances have forced strong changes in the structure in addition to the variation of the CCNS dihedral angle. Both minima are SMX-syn conformers, SMX-synM1 (Fig. 3c) and SMX-synM2 (Fig. 4b) have similar energy, being this last one the most stable $\Delta E = 0.064$ kcal/mol, although the rotational barrier is around 3.9 kcal/mol. Both conformers can be considered the same structure and the only difference is the relative orientation of the NH_2 H atoms of the aromatic ring (Fig. 4b). On the other hand, the HNSO dihedral angle scan with the rotation of the S-N bond showed also other two minima (Fig. 4c). Both minima, SMX-synM1 (Fig. 3c) and

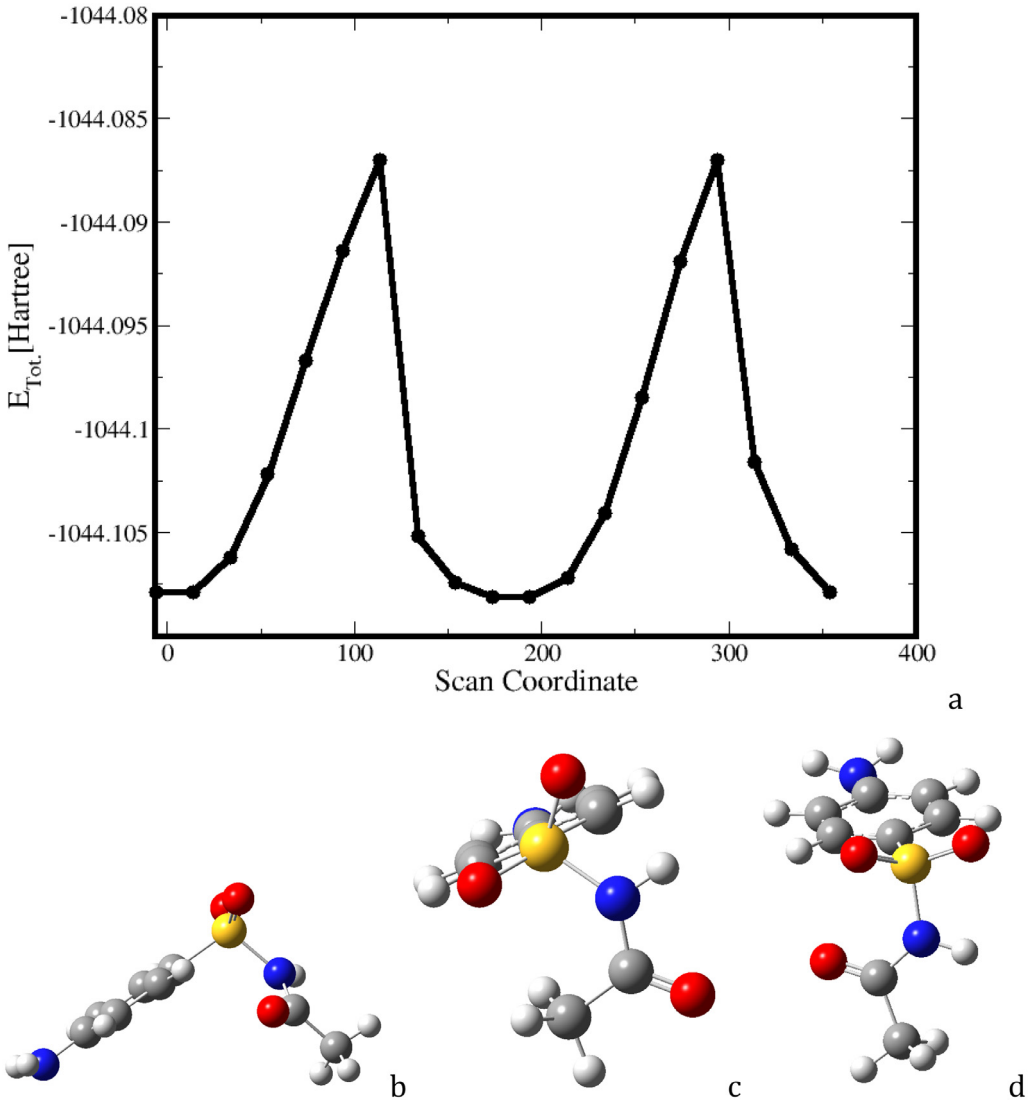

Fig. 6. Scanning of the SNCO dihedral angle of SCM (a), and the optimized minima SCM-M1 (b), SCM-M1 (syn) viewed from the sulfoxide group in a perpendicular plane of the H_2N-S axis (c), and SCM-M2 (anti) (d).

SMX-synM3 (Fig. 4d), are also syn conformers with similar energy, being the most stable the SMX-synM3 with $\Delta E = 0.137$ kcal/mol, although the rotational barrier is high, around 6 kcal/mol. The energy difference is small and they can be considered the same structure. Calculations based on GGA/PBE yielded similar results being more stable the syn conformer with a higher energy difference (Table S1, in Supplementary Support).

In the SCP molecule two main conformers can be distinguished. A scan of the dihedral angle S-N-C–C with the rotation of the N–C bond, two minima can be considered (Fig. 5). The conformer syn (SCP-M1) where the N–H bond is oriented to the same side of the heterocyclic N atoms, and the conformer anti (SCP-M2) where the N–H is oriented to the opposite side of the N–N bond (Fig. 5). The conformer SCP-M1 (syn) is 3.40 kcal/mol more stable than SCP-M2 (anti). Similar results were obtained at GGA/PBE level (Table S1).

In SCM two conformers can be also distinguished during the rotation of the dihedral angle S-N-C = O, the conformer syn (SCM-M1), where the N–H bond is oriented at the same side of the carbonyl group, and the anti one (SCM-M2) where both groups, N–H and C = O are in opposite side. Both conformers have similar energy with a rotation barrier of 13.5 kcal/mol (Fig. 6). Sharp peaks are observed in this profile, indicating that additional changes are produced in addition to the rotation of the dihedral angle S-N-C = O, In GGA/PBE calculations, the syn conformer is more stable, 1.65 kcal/mol, than the anti one (Table S1).

The main geometrical features of the molecule structures optimized are compared with experimental data in Table 1. In general, the main geometry features are consistent with the experimental values. The calculated values are from isolated molecules, whereas the experimental values are from crystal structures. The intermolecular interactions in the molecular crystal can justify the differences in some experimental and calculated values. Besides, some variations were observed in the experimental data depending on the authors and the polymorph crystal structure. The S-O bond close to the N–H bond is slightly longer in SMT and the anti conformers of SMX, SCP and SCM than in the syn conformers. At the same time, the syn conformers have longer S-N and N–C bonds and higher O-S-O and smaller S-N-H bond angles than in the anti conformers, due to interactions between the N–H and S = O groups. However, this interaction is not through hydrogen bonds, because the NH…OS distance is higher in syn than in anti conformers. Hence, this interaction can be electrostatic. These differences are not observed in SCM where more freedom degrees exist. The experimental values of S-O, S-N bonds are slightly shorter

Table 1
Main geometrical features (distances in Å and angles in º), relative energy (in kcal/mol) and dipole moment (D) of the sulfonamide molecules optimized at M06–2X/6–311+G(d,p) level.

	SMT[a,b]	SMX syn[c]	SMX syn[d]	SMX anti	SCP syn[e]	SCP anti[e]	SCM syn	SCM anti
ΔE[f]	–	0.0	–	1.83	0.0	3.4	0.0	0.1
ΔG[f]	–	0.0	–	1.68	0.0		0.0	0.5
μ	13.67	10.31	6.62	9.00	8.03	8.32	10.86	9.90
S-O_1	1.461 (1.435[a],1.430[b])	1.456 (1.441)	1.447	1.460	1.455 (1.434)	1.460	1.457	1.459
S-O_2	1.454 (1.431[a],1.426[b])	1.455 (1.435)	1.445	1.457	1.455 (1.433)	1.456	1.453	1.454
S-C	1.755 (1.746[a],1.765[b])	1.751 (1.747)	1.767	1.749	1.751 (1.734)	1.750	1.751	1.749
S-N	1.678 (1.632[a,b])	1.689 (1.651)	1.688	1.671	1.694 (1.647)	1.675	1.681	1.683
N-C	1.405 (1.406[a],1.412[b])	1.403 (1.407)	1.399	1.389	1.413 (1.394)	1.391	1.392	1.382
NC-N_{het}	1.328 (1.333[a],1.343[b])	1.306 (1.307)	1.304	1.306	1.322 (1.324)	1.320	1.216[g]	1.217[g]
N-O		1.381 (1.414)	1.377	1.389	1.328[g]	1.333[g]		
O-C		1.350 (1.356)	1.341	1.350	1.735[g]	1.740[g]		
N-H…OS	2.45 (2.35[a], 2.54[b])	2.56 (2.48)	2.48	2.48	2.56 (2.43)	2.45	2.48	2.49
O-S-O	117.8 (119.0[a],118.0[b])	119.7 (119.4)	122.7	118.0	119.7 (119.4)	118.1	119.0	119.0
S-N-H	111.2 (111.8[a],119.5[b])	109.7 (113.2)	111.2	113.0	108.6 (114.2)	112.6	113.5	115.2
C-S-N	106.8 (108.2[a],107.2[b])	106.9 (107.1)	106.1	104.8	106.6 (106.7)	106.0	106.6	106.7
C-S-N-C	42.8 (83.0[a],84.9[b])	52.8 (55.0)	58.6	71.3	52.3 (63.5)	75.0	61.7	58.0
C-C-S-N	61.9 (55.0[a,b])	85.5 (74.8)	88.0	66.2	91.5 (77.7)	66.8	59.5	78.6
S-N-C-N_{het}	150.6 (146.2[a],148.3[b])	126.4 (140.7)	130.0	17.0	116.9 (85)	22.0	167.0[h]	6.2[h]
H-N-C-N	9.5 (17.3[a], 27.4[b])	1.9 (2.1)	3.1	165.1	8.3 (4.4)	172.7	7.6 [h]	173.5[h]
H_2N-S-C_{het}[i]	74.9 (102.0[a],101.6[b])	85.8 (81.0)	84.5	94.2	85.6 (87.0)	98.4	94.5	96.5
C-C'-N-X[j]	0.5 (18.5[a], 36.5[b])	1.9 (8.7)	6.9	20.9	39.0 (16.4)	19.7	0.9	35.5

[a] Values in brackets are experimental data from ref. 13.
[b] Experimental data from ref. 14.
[c] In brackets experimental data from ref. [34].
[d] In gas phase without solvent.
[e] In brackets experimental data from ref. 16.
[f] Energy in kcal/mol with respect to the minimum one; ΔE is corrected with the zero point energy and ΔG is corrected with the thermal free energy at 298 K.
[g] N–N bond length and C–Cl bond length.
[h] Carbonyl O atom instead of heterocyclic N atom.
[i] Angle between both rings.
[j] Coplanarity of both rings, both aromatic C atoms in alpha position with respect to the sulfoxide group and the heterocyclic N atoms in SMT and heterocyclic N and C atoms in SMX.

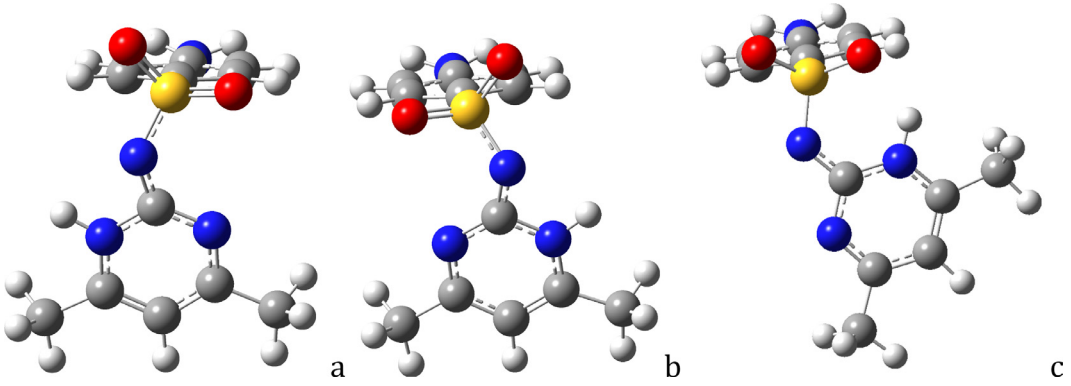

Fig. 7. Optimized structures of the N-sulfonimide tautomeric forms of SMT, SMT-M1_t (a), SMT-M2_t (b), and SMT-M3_t (c).

than the calculated. These theoretical values are calculated in a water media polarizing and enlarging the S = O bond, whereas the experimental values are from crystal structures. In the SMX molecule optimized in gas phase without solvent, the S = O bonds are shorter and closer to the experimental. The S-C bond is slightly shorter in SMX than in SMT indicating a higher electronic connection between the aminoaryl moiety and sulfoxy group. In SMT this bond length is within the experimental range values depending on the crystal structure. However, this calculated bond length is slightly longer than the experimental values. Probably the intermolecular interactions of the sulfoxide group in the crystal lattice polarize the S = O bond increasing the bond order in S-C by resonance decreasing the bond length. In the isolated SMX molecule without intermolecular interactions, this S-C bond is longer than in water or in crystal, minimizing the electronic transmission between the aromatic ring and sulfoxide group. Similar behavior is

Table 2
Main geometrical features (distances in Å and angles in º), relative energy (in kcal/mol) and dipole moment (D) of the sulfonimide tautomer forms.

	SMT_t	SMX_{syn}_t	SMX_{anti}_t	SCP_{syn}_t	SCP_{anti}-t	SCM_{anti}_t	SCM_{syn}_t
ΔE[a]	1.03 (37.7)	7.07 (53.0)	5.40	1.52 (38.8)	1.15	7.92	7.37 (38.5)
ΔG[a]	0.86	6.66	5.57	2.00	1.60	8.37	8.39
μ	16.89	14.05	13.32	12.15	11.25	13.63	14.77
$d(S\text{-}O_1)$	1.465	1466	1.464	1.465	1.462	1.463	1.465
$d(S\text{-}O_2)$	1.479	1.471	1.475	1.470	1.475	1.466	1.462
d(S-C)	1.767	1.768	1.765	1.767	1.763	1.760	1.761
d(S-N)	1.617	1.627	1.631	1.630	1.633	1.671	1.658
d(N–C)	1.333	1.320	1.322	1.320	1.321	1.289	1.290
d(N–H)	1.021	1.016	1.017	1.017	1.018	0.969[g]	0.968[g]
$d(C\text{–}N_1)$	1.347	1.355	1.356	1.359	1.358	1.325[g]	1.328[g]
d(N–O)		1.375	1.378				
d(O–C)		1.352	1.357				
N-H…OS	2.013	–	2.199	2.464	2.080		
(O-S-O)	115.9	116.1	116.6	116.1	116.6	116.7	116.6
(C-S-N)	106.7	107.2	106.6	107.0	106.1	107.5	107.4
C-S-N–C	73.3	66.4	75.3	66.2	75.7	63.4	56.4
C–C-S-N	74.4	66.1	74.9	62.9	73.3	76.2	58.4
$S\text{-}N\text{-}C\text{–}N_{het}$	168.5	174.7	1.7	177.9	6.6	0.6[g]	178.7[g]
H-N-C–N	5.1	30.4	32.6	177.8	5.6		
$H_2N\text{-}S\text{-}C_{het}$[b]	89.0	93.7	93.6	87.8	89.2	98.6	97.9
C-C'-N-X[c]	1.5	23.2	3.5	7.1	13.9	40.0	13.4

[a] Relative energy in kcal/mol with respect to the minimum sulfonamide tautomer; the tautomerism energy barrier is in brackets.
[b] Angle between both rings.
[c] Coplanarity of both rings, both aromatic C atoms in alpha position with respect to the sulfoxide group and the heterocyclic N atoms in SMT and heterocyclic N and C atoms in SMX.
[g] Carbonyl O atom instead of heterocyclic N atom.

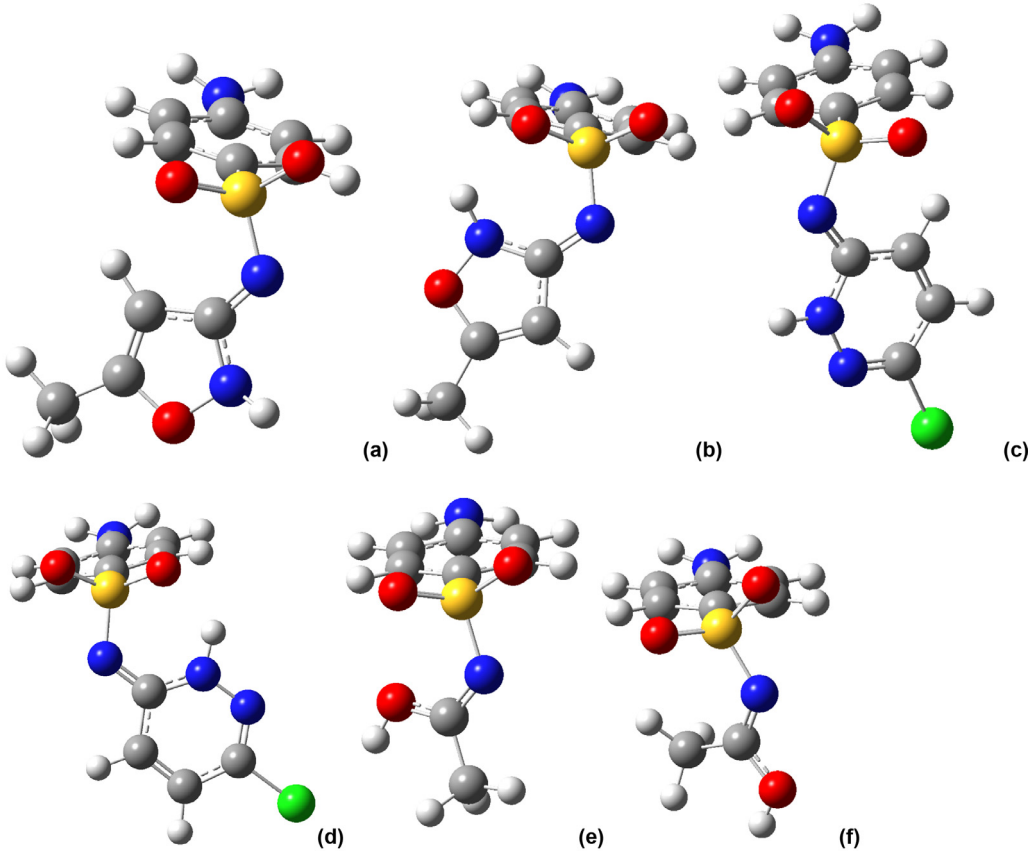

Fig. 8. Optimized N-sulfonimide tautomeric forms of SMXsyn (SMXsyn_t) (a), SMXanti (SMXanti_t) (b), SCPsyn (SCPsyn_t) (c), SCPanti (SCPanti_t) (d), SCManti (SCManti_t) (e), and SCMsyn (SCMsyn_t) (f).

Table 3
Cell parameters of the calculated and experimental (in brackets) crystal structures of SMT (distances in Å and angles in º).

SMT	*a*	*b*	*c*	*α*	*β*	*γ*
SLFNMD01	7.46 (7.43)	18.79 (18.99)	9.26 (9.32)	90.0 (90.0)	99.7 (99.1)	90.0 (90.0)
SLFNMD10	7.52 (7.46)	18.69 (18.94)	9.25 (9.27)	90.0 (90.0)	99.3 (97.3)	90.0 (90.0)

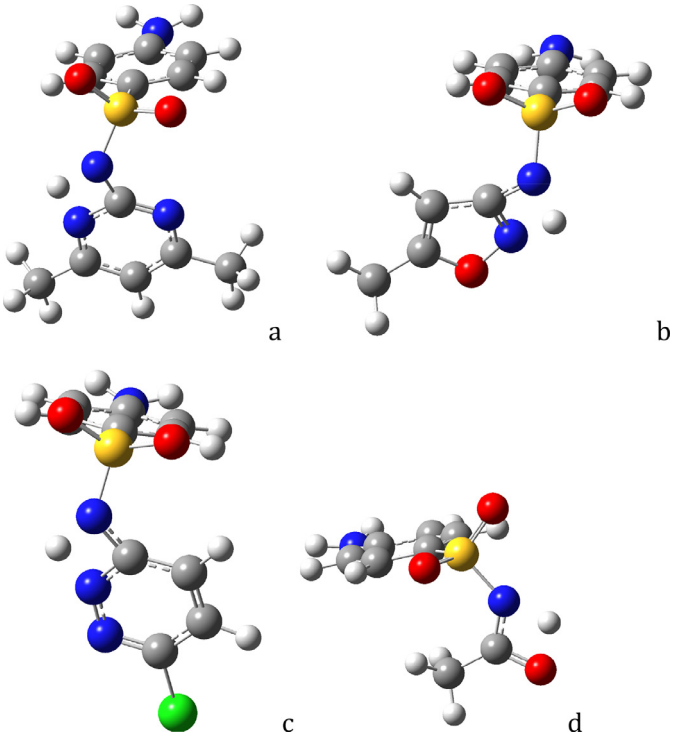

Fig 9. Transition states of the intramolecular proton transfer between tautomeric forms of the sulfonamide-sulfonimide tautomerism in SMT (a), SMXsyn (b), SCPsyn (c), and SCM (d).

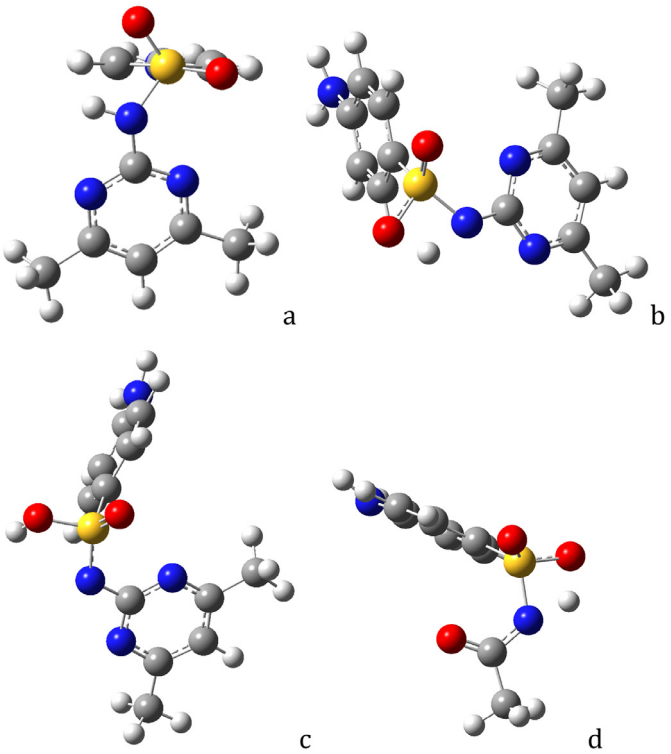

Fig. 10. Intramolecular proton transfer between the N–H group and the sulfonyl moiety in the sulphonamide keto (a)-enol (c) through the TS (b). TS in this proton transfer of SCM (d).

observed in the C–N bond. In this bond, the differences between experimental and calculated values are higher, because the intermolecular interactions of the CN–H group are very strong in the crystal lattice. The angle H_2N-S-C_{het} indicates the angle between the axes of both rings, and is close or smaller than 100º in all cases. In SMX and SCM, the conformer anti have lower dipole moment and probably the population of these conformers can increase in non-polar environments overcoming the energy differences with the more polar syn conformers.

Some differences are observed in the dihedral angles. The C-S-N–C angle in the calculated molecules is smaller than in experimental data of solids, due to the intermolecular interactions in the crystal lattice. This is confirmed with the value in the calculated crystal structure of SMT that reproduces the experiment (Table S1). Both rings (aromatic and heterocyclic) are coplanar in SMT, SMXsyn, and SCMsyn (low values of the C–C'-N-X dihedral angle) with the ring axes forming angles close to 100º, being slightly twisted in SMXanti, SCP and SCManti models. The same behavior is observed in the main molecular geometry features calculated at GGA/PBE level (Table S1).

4.2. Tautomerism in sulphonamide molecules

The arylsulfonamides with heterocyclic N atoms can exhibit tautomerism between the sulfonamide and sulfonimide forms [6]. These tautomers can be present in the biological system and are active in their therapeutic use. In the crystal structures of these sulfonamides, the N-sulfonimide forms can exist in these crystal lattice structures and can be responsible of the crystal polymorphism of these sulfonamides. Since the sulfonamide group, -SO_2NH-R is an acidic moiety that is found in a lot of pharmaceutical, veterinary and agrochemical compounds, such that the arrangements in the tautomeric structures are different and some physicochemical properties change with respect to the nature of the substituents. Therefore, the tautomeric structures of sulfonamides play an important role in the biological and synthetic applications. Besides, this tautomerism should be taken into account in the interactions of these drugs with biopolymers, such as, proteins, and DNA [34].

We have optimized the tautomeric forms in the same calculation conditions as above. In SMT several conformers can be distinguished in the sulfonamide tautomers, coming from the conformers of SMT (Fig. 2), SMT-M1_t and SMT-M2_t that have similar energy (ΔE = 0.1 kcal/mol); and another with N–H oriented to one sulfonyl O atom SMT-M3_t that has more energy (ΔE = 1.9 kcal/mol) and it is less probable (Fig. 7). In all cases, the sulfonamide tautomer is more stable than the sulfonimide forms (SMT_t) (Table 2). In SMX two conformers can be distinguished in the sulfonimide tautomer, SMXsyn_t and SMXanti_t corresponding to those in the sulfonamide form. The most stable conformer is SMXanti_t, being only 1.67 kcal/mol more stable than the con-

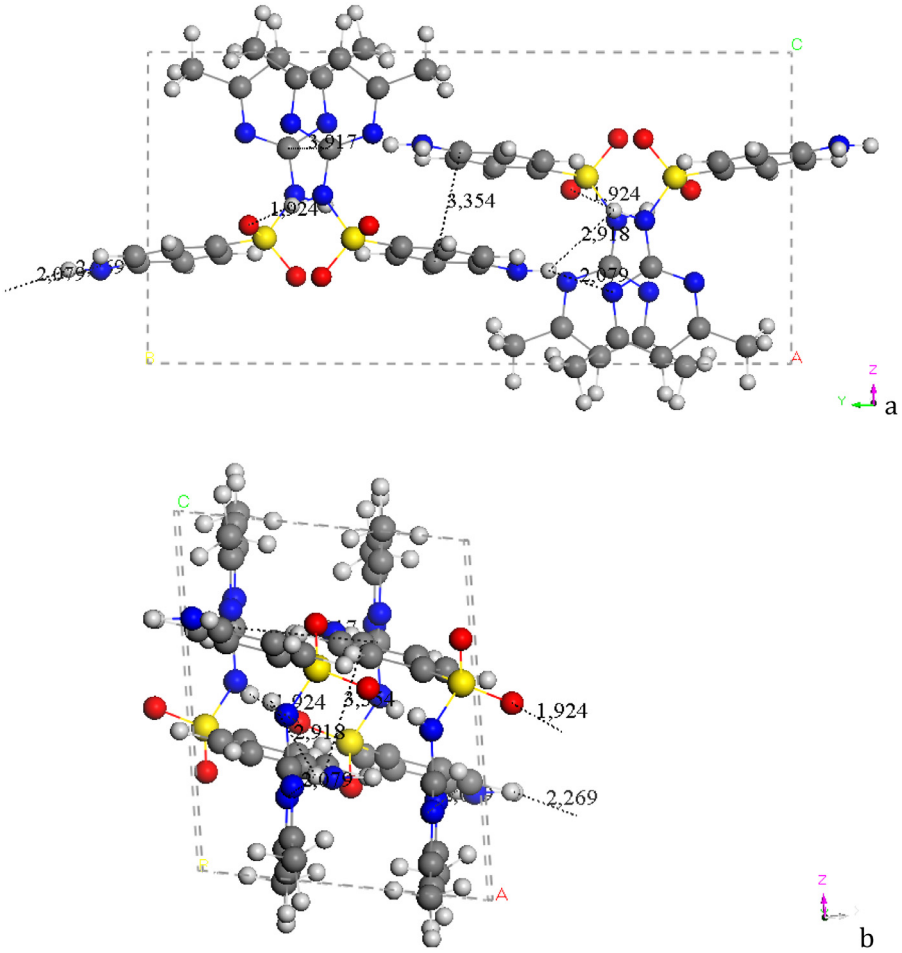

Fig. 11. Optimized crystal structure of sulfamethazine. Views from (100) (a) and (010) (b) planes.

former syn. This is the opposite that found in the sulfonamide tautomers, due to the intramolecular H bond between the heterocyclic N–H group and one sulfoxy O atom, d(N.H···OS) = 2.199 Å. The sulfonamide tautomer of SMX_syn is 5.40 kcal/mol more stable than the sulfonimide form SMX_anti_t. In SCP two conformers can be distinguished also, syn and anti. The SCPanti_t is 0.37 kcal/mol more stable than SCPsyn_t. The contrary behavior was found above in the conformers of the sulfonamide tautomer. In the sulfonimide tautomer SCPanti_t the intramolecular interaction between de N–H group and one sulfoxy O atom d(N–H···OS) = 2.080 Å is stronger than in the syn conformer. In SCM the tautomerism is different, being of keto-enol type instead of NH exchange (Fig. 8). The SCManti_t has higher energy than SCMsyn_t. The sulfonamide tautomer is 7.37 kcal/mol more stable than the sulfonimide form SCMsyn_t. In the QE calculations, the relative tendency between conformers is similar being the energy differences higher.

The sulfonimide tautomers are more polar than the sulfonamide ones (Table 2). The S = O bond lengths are longer than in the sulfonamide tautomers, especially those that have intramolecular interaction with the N–H group. In the sulfonimide tautomers the S-C bond is slightly longer than in the sulfonamide forms. On the contrary, the S-N and N–C bonds are shorter in the sulfonimide tautomers than in the sulfonamide forms. This indicates that a delocalization of electrons is produced between the N atoms and sulfoxide O atoms. The C–N bonds in the heterocyclic moieties are longer in the sulfonamide tautomers due to the N–H form.

In general, the sulfonamide tautomers are more stable than the sulfonimide forms. Nevertheless, these energy differences are not drastic, especially in SMT and SCP. We have explored the reaction path of the transposition of the H atom between both forms finding the transition state (TS). In all cases, this TS showed only one negative frequency that corresponds to the transition of this H atom vibrating between both N atoms. The activation energy of this tautomerism is defined by the energy barrier between reactants and TS, being very high in all cases (Table 2). In all TS's, the H atom is localized in an intermediate position between both N atoms in a 2.2–4.1 Å range (Fig. 9).

Another kind of tautomerism can be observed in these molecules related with the keto (sulfonyl) and enol (thioenol) forms of sulfonamide tautomers, where an intramolecular proton transfer occurs between the heterocyclic N–H group and the sulfonyl moiety [35]. This interaction is interesting because can be observed at intermolecular level in some crystal structures of sulfonamides. The keto form of SMT is much more stable than the enol form with higher energy differences (ΔE = 20.45 kcal/mol; ΔG = 19.77 kcal/mol) than in the sulfonamide-sulfonimide tautomerism. Similar values have been found for SCM. We have explored the reaction path of the intramolecular proton transfer between both forms finding the transition state (TS) that showed only one negative frequency corresponding to the proton transition. The activation energy of this tautomerism in SMT is 41.09 kcal/mol (ΔG = 40.06 kcal/mol) (Fig. 10). Similar energy barrier was found in SCM (Fig. 10). This is consistent with similar tautomerism in other sulfonamides [35]. These higher energy differences indicate that these enol tautomers are less probable.

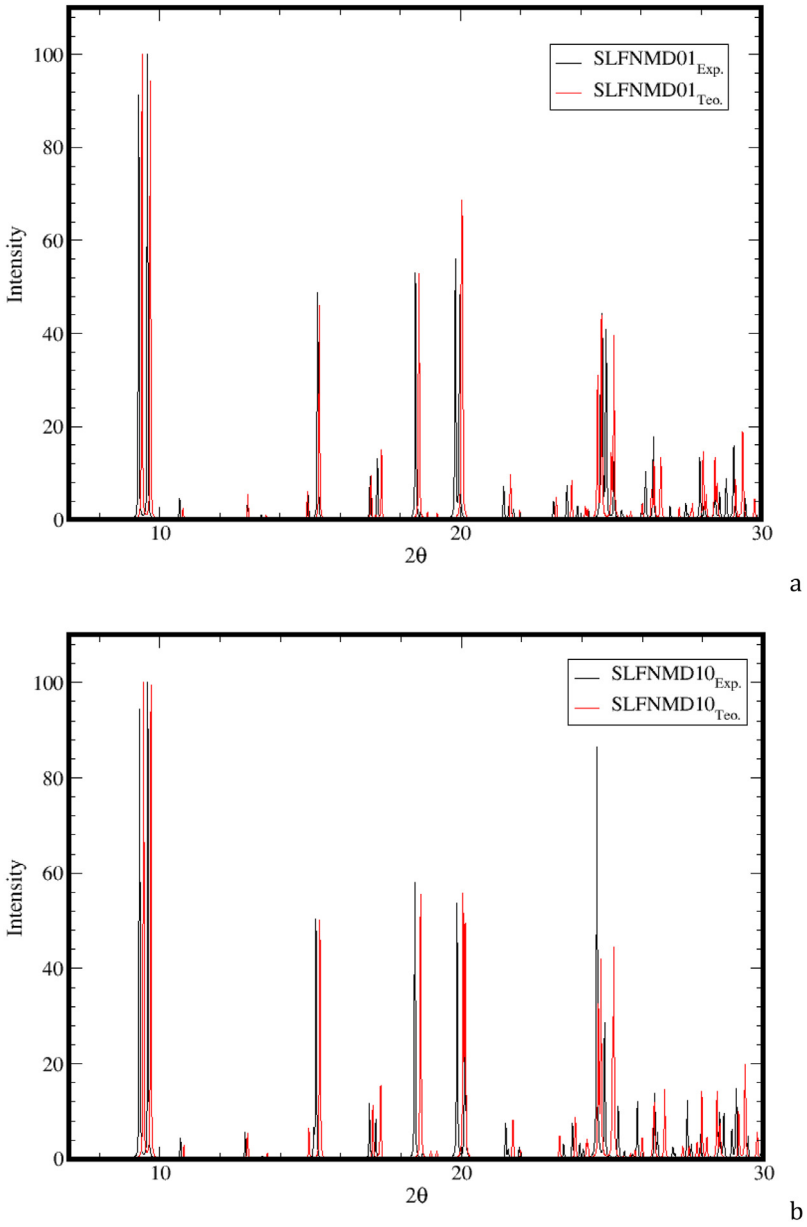

Fig. 12. Powder X-ray diffraction patterns simulated from the crystal structures SLFNMD01 (a), SLFNMD10 (b) of sulfamethazine.

4.3. Sulfonamide crystal structures

Before exploring the spectroscopical properties of these drugs, we have to consider that many infrared analysis are performed at solid state, where the drugs are in crystalline state. Hence, we have to study the crystal structure where the intermolecular interactions are responsible to the frequencies of the main functional groups.

In the case of sulfamethazine, three crystal forms have been claimed based on x-ray diffraction, CCDC num.1260687, code: SLFNMD01 [13]; CCDC num. 1,260,688, code: SLFNMD02 [15]; and CCDC num. 1,260,689, code: SLFNMD10 [14]. Mesley and Houghton [36] claimed two polymorphs I and II based on IR spectroscopy. The form II was obtained from the form I by trituration. However, their IR spectra, thermograms and X-ray diffractograms were too similar and the distinction was not clear [7]. Nevertheless, Kuhnert-Brandstatter and Wunsch [37] reported four forms of sulfamethazine by thermomicroscopic methods without solid characterizations. However, Maury et al. [15] reported the existence of only one polymorph and different crystal habits. One of the aims of this work is to clarify these controversies.

The only atomic coordinates available are SLFNMD01 and SLFNMD10. Both are similar with different refinement accuracy. We optimized the crystal structures SLFNMD01 and SLFNMD10 with QE reproducing the experimental crystal lattice parameters (Table 3). Taking into account that the unit cell is formed by 4 molecules of SMT and comparing the energy of the unit cell with the energy of the isolated molecule, the cohesive energy of this crystal is −41.30 and −41.38 kcal/mol per molecule in the optimized SLFNMD01 and SLFNMD10 respectively. Both structures have similar energy. The main interatomic distances are described in Table S1. The aromatic rings are parallel at 3.35 Å with a shift where the amino groups are over the vicinal aromatic π-electron cloud (Fig. 11a). The heterocyclic rings are also parallel at 3.92 Å and slightly shifted for avoiding the repulsion interactions between the heterocyclic N atoms (Fig. 11b). The π-π interactions between both types of rings facilitate the packing in this crystal. The N–H group

Table 4
Calculated and experimental IR frequencies (cm^{-1}) of SMT.

Mode [a]	SMT	SMT[b]	SMT_{QE}[c]	SMT_{exp}[d,e]	SMT_{crys}[c,f]
$\nu(NH_2)_{as}$	3695	3724	3624	3423, 3450[e]	3500, 3498
$\nu(NH_2)_s$	3582	3617	3500	3355, 3370[e]	3315, 3304, 3300, 3296
ν(NH)	3557	3610	3520	3259, 3250[e]	3300, 3293
ν(CH)arom	3234[g,h]	3246_{as}[g,h]	3147	3102, 3100[e]	3130–3129[g,j], 3128–3127_s[h], 3119–3117_{as}[h]
ν(CH)het	3222	3211	3120	3075, 3085[e]	3175, 3174,
ν(CH)arom	3213[i,j], 3194[h,i], 3184[g,j]	3213_s[j], 3195[h,i],3199_{as}[j]	3127 3095, 3099	3066–3039, 3060–3030[e]	3094–3093
$\nu(CH)_{as}$ CH_3	3168[h], 3161[j], 3136[h], 3133[j]	3167[h], 3169[j], 3137[h], 3140[j]	3066, 3062, 3036, 3028	2920[e]	3077- 3034
$\nu(CH)_s$ CH_3	3064[h], 3063[j]	3067	2976, 2971	2900[e]	3093, 2992, 2968
Ring het	1675, 1622, 1257	1668, 1648, 1255	1557	1585, 1660[e]	1582–1571
Ring arom	1661, 1642	1683, 1656	1606, 1592	1594, 1580, 1615[e]	1603–1595
$\delta(NH_2)_s$	1620	1658	1543	1652, 1605[e]	1633, 1630–1628
δ(CH)arom	1541	1553	1487	1501, 1492, 1560[e]	1544, 1498
δ(CH)het+ δ(NH)	1526	1527	1443, 1236	1408, 1510[e]	1454–1451, 1402–1392
$\delta(CH_3)_s$	1484	1425, 1411	1430	1480[e]	1442
$\delta(CH_3)_{as}$	1468–1457	1501–1482	1419–1414	1420[e]	1435, 1416
ν(CN)	1449, 1343[k]	1330	1423, 1314	1262,1304[k], 1390[e]	1533–1495, 1257–1242, 1073, 1392[k]
$\delta(CH_3)$umb	1399, 1384		1353,1324	1330–1300[e]	1364–1349, 1333–1329, 1325, 1241
δ(CH)het	1205	1194	1153	1093, 1190[e]	1171
δ(CH)arom	1207, 1155	1340, 1334, 1214, 1155	1314, 1171, 1117	1187, 1160–1130[e]	1294, 1179, 1127
$\nu(SO)_{as}$	1281		1318	1326, 1300[e]	1257–1242
$\nu(SC) + \nu(SO)_s$	1138	1175	1116, 1055	1157, 1100[e]	1101–1096, 1057–1051
$\delta(NH_2)_{as}$	1077	1085	1020	1080[e]	1126, 1036–1033
$\gamma(CH_3)$	1063, 1056	1066, 1061	1017, 1009	980[e]	1021–1008
ν(NS)		873			
γ(CH)het	879	854	932, 827	971, 880[e]	844–840
γ(CH)arom			943	971, 880[e]	961–948

[a] Normal vibration modes, *as*=asymmetric, *s*= symmetric, arom=aromatic, het=heterocyclic, umb=umbrella.
[b] Values for the isolated molecules calculated in gas phase.
[c] Calculated with GGA/PBE.
[d] Experimental data in solid state with KBr of sulfadiazine, a similar structure without methyl groups [38].
[e] Values extracted from the experimental spectrum of SMT in solid state with KBr [15] no assignment was reported.
[f] Values calculated from the optimized crystal structure.
[g] In alpha position with respect to the SO group.
[h] In the anti zone with respect to the N–H bond.
[i] In alpha position with respect to the amino group.
[j] In the zone syn with respect to the N–H bond.
[k] CNH_2.

forms a strong H bond, d(NH…OS) = 1.924 Å, with the sulfoxy O atom. The amino H atoms form H bonds with the heterocyclic N atoms of different vicinal molecules, d(NH…N) = 2.079, 2.269 Å. These interactions indicate the tendency to form the sulfonimide-sulfonamide tautomers that have low energy difference in SMT (Table 2). Notice that some dihedral angles change during crystallization. The C-S-N–C angle is smaller in the molecule than in the calculated crystal (Table S1). The H–N-C–N and C_α-C'$_\alpha$-N-X angles are larger in crystal than in molecular structures losing a certain grade of coplanarity. Besides, the molecules are more open in crystal structure than isolated increasing the H_2N-S-C_{het} angle (Table S1). All these comparisons have been confirmed with the experimental data (Table 1).

The XRD patterns of these structures were simulated observing all patterns are similar indicating that these structures are the same polymorph (Fig. 11). Hence, only one polymorph is present in this SMT (Fig. 12).

4.4. Spectroscopical properties

The vibrational spectroscopy is one experimental technique that represents vibrational atomic movements; hence it is close to atomic theoretical calculations. Then, we calculated the main vibrational normal modes of these molecules for comparison with the few experimental data (Tables 4-7). Besides, we study the effect of conformational changes on the frequencies and the differences produced with tautomerism (Tables 8 and S3). Although there are only experimental data for some of these sulphonamides, in general, the calculated frequencies are higher than the experimental values. These differences are due to the harmonic approximation of the calculations and also to the interatomic interactions that do not exist in the molecules models. This fact is smaller with aqueous solvent effect than in gas phase. These differences are smaller using GGA/PBE approach than using the M06–2X functional. Nevertheless, these differences follow a linear relationship being possible to apply a factor scale of 0.944 for gas phase calculations [12], 0.955 for M06–2X calculations with water effect, and 0.985 for GGA/PBE calculations. This means that the frequencies calculated with QE are closer to experimental values.

In SMT the frequencies of the vibration modes of polar groups, as NH, SO and NH_2, calculated in gas phase are higher than those calculated with the aqueous solvent effect. These polarizable groups are more sensitive to the environmental changes as the solvent. Some differences in the ν(CH) vibration mode of the C–H bonds of the aromatic aminobenzenic ring, depending on their positions with respect to the amino or sulfoxy groups and the N–H bond. So, the C–H bond close to the S = O bond shows higher frequency than others, due to the local electric field produced by the

Table 5
Calculated IR frequencies (cm^{-1}) of SMX along with experimental data.

Mode [a]	SMX_{anti}	SMX_{syn}	SMX_{syn} [b]	SMX_{antiQE}	SMX_{synQE}	SMX_{exp} [o]
$\nu(NH_2)_{as}$	3698	3701	3734	3633	3644	3462
$\nu(NH_2)_s$	3584	3587	3624	3520	3531	3376
ν(NH)	3549	3492	3558	3493	3458	3292
ν(CH)arom	3226_{as}[c,d]	3209_s[f]	3206[f]	3140	3137	
ν(CH)het	3282	3295	3298	3186	3214	
ν(CH)arom	3208_s[f]	3199_{as}[d]	3191[d]	3125	3125	
ν(CH)arom	3194[d,e]	3195_{as}[f], 3212_s[d]	3192[f], 3231[d]	3106	3100, 3097	
	3192_{as}[f]			3092		
$\nu(CH)_{as}$ CH_3	3172, 3138	3180, 3137	3163, 3136	3079, 3039	3073, 3032	
$\nu(CH)_s$ CH_3	3066	3068	3066	2983	2979	
Ring het	1692, 1592[g]	1685, 1583,1504	1693	1601	1601, 1246	1640
Ring arom	1655, 1640,	1657, 1637	1684, 1653	1605, 1550, 1351	1557, 1488	1610
$\delta(NH_2)_s$	1620	1621	1657	1589	1592	1500
δ(CH)arom	1542, 1481	1536, 1483	1550, 1485	1551	1431	
δ(CH)het+ δ(NH)	1522			1477, 1279, 1225	1467	
$\delta(CH_3)_{as}$	1464, 1455	1457, 1454, 1331	1484, 1479	1428	1419, 1359	
ν(CN)	1347[h]	1504	1519, 1337[h]	1446, 1315[h]	1457, 1316[h]	
$\delta(CH_3)$umb	1402	1405	1412	1358	1357	
δ(CH)het	1334, 1159	1162	1163	1129	1127	
δ(CH)arom	1209, 1157	1369, 1346, 1205, 1155	1362, 1334, 1214, 1156	1291, 1171, 1116	1288, 1171, 1116	
δ(NH)	1368	1390	1418		1331, 1264	
$\nu(SO)_{as}$	1281	1298		1279	1246	1317
$\nu(SC) + \nu(SO)_s$	1140, 1103	1141, 1103	1183, 1120	1111, 1059	1113, 1062	1317
ν(XO)	1084[k]	1274[m], 1069[k]	1324[m], 1090[k]			
$\delta(NH_2)_{as}$	1080	1078	1080	998	1016	
$\gamma(CH_3)$	1061	1066	1066	1018	1019	
ν(NS)	870	897	898			1157
γ(CH)het	804	998[j], 978[j]	998[j].980[j]			929, 828

[a] Normal vibration modes, as=asymmetric, *s*= symmetric, arom=aromatic, het=heterocyclic, umb=umbrella.
[b] Values for the isolated molecules in gas phase.
[c] In alpha position with respect to the SO group.
[d] In the anti zone with respect to the N–H bond.
[e] In alpha position with respect to the amino group.
[f] In the zone syn with respect to the N–H bond.
[g] ν(CN) coupled with other heterocyclic ring vibrations.
[h] CNH_2.[i]Amide group.
[j] Aromatic ring.
[k] ν(NO).
[m] ν(CO) vibration mode.
[o] Experimental data from ref 39.

S = O dipole. This effect is slightly stronger when the C–H bond is in the orientation anti with respect to the N–H group and the C–H and S = O bonds are co-planar (Fig. 3). In the region of lower frequencies than 1683 cm^{-1}, a series of vibration modes appear overlapping each other. We have grouped the main modes, ν(CC), ν(CN), δ(CH), as ring vibrations for the aminobenzenic and heterocyclic rings. At lower frequencies region, we have highlighted those vibration modes that can be distinguished. The frequencies calculated for the molecules optimized at the M06–2X level of theory follow a similar trend that those calculated with QE with some small differences. The ν(NH) frequency is higher than $\nu(NH_2)_s$ with QE, whereas the contrary is observed with M06–2X. However, in the crystal packing these vibration modes appear at similar frequencies, due to the coupling of the vibrations of similar functional groups of different molecules within the crystal lattice. The frequencies of the $\nu(NH_2)_s$ and $\nu(NH_2)_{as}$ modes are lower in experimental data than in the calculated isolated molecules, due to the intermolecular hydrogen bonds of the N–H group with the heterocyclic N atom and the amino NH_2 group with the sulfonyl O atom existing in the crystal packing. This is corroborated with the frequencies of these groups in the calculated crystal structure of SMT (Table 4). The modes corresponding to the 1600–1000 cm^{-1} range are highly coupled between the molecules packed in the crystal lattice.

In SMX, the same behavior as SMT was found in the frequencies differences of including the aqueous solvent effect and between the M06–2X and QE calculations. The main vibration modes of the polar groups, NH, NH_2, and SO, appear at higher frequencies in gas phase than in aqueous media, as in SMT. The vibration mode ν(NH) has higher frequency in the conformer anti than in syn. This can be owing to a higher effect of the local electric field of the S = O dipole on the N–H bond that is closer in the conformer anti than in syn (Table 2). The same effect can justify that the ν(NH) frequency in SMT is slightly higher than in SMX, because the N–H bond is closer to the S = O group in SMT than in SMX. The same differences in the ν(CH) vibration modes of the aromatic aminobenzenic ring observed in SMT were found in SMX. In all cases, conformers and calculation types, the ν(NH) mode appears at lower frequency than $\nu(NH_2)_s$ mode. The ν(CH) of the heterocyclic C–H bond in the conformer syn appears at higher frequency than in anti, because the effect of S = O dipole is higher in syn (Fig. 4). The bending δ(NH) mode appears at higher frequency in syn than in anti, due to the higher local electric effect in syn, where the N–H bond has to vibrate between two dipoles, S = O and C–N.

In SCP, the same frequency differences in the $\nu(NH_2)$ and ν(NH) modes between conformers syn and anti, observed above in SMX, were shown also in SCP (Table 6). Similar effect is observed in SCM (Table 7).

The IR frequencies of the sulfonimide tautomers were also calculated (Table 8) (Table S3). The $\nu(NH_2)$ vibration modes are similar to the sulfonamide tautomers. However, the ν(NH) shows dif-

Table 6
Calculated IR frequencies (cm^{-1}) of SCP.

Mode [a]	SCP_{syn}	SCP_{anti}	SCP_{exp} [b]	SCP_{synQE}	SCP_{antiQE}
$\nu(NH_2)_{as}$	3708	3700	3494	3632	3630
$\nu(NH_2)_s$	3592	3587	3392	3517	3519
ν(NH)	3493	3580	3248	3439	3526
ν(CH)het	3240_s, 3229_{as}	3236_s, 3215_{as}		3143_s 3129_{as}	3125_s, 3103_{as}
ν(CH)arom	3219_s[f], 3214_s[d], 3203_{as}[d], 3196_{as}[f]	3227_s[d], 3210_s[f], 3198[e], 3195		3129_s[f] 3102_{as}[f] 3098_{as}[d]	3156[c,d], 3124_s[f], 3107[d], 3101_{as}[f]
Ring het	1650, 1637	1664, 1637	1574	1565, 1562, 1532	1562, 1519
Ring arom	1655, 1636	1659, 1645	1595	1565, 1562	1551, 1487, 1430
$\delta(NH_2)_s$	1621	1626	1625	1608, 1592	1603, 1589
δ(CH)arom	1537, 1482	1545, 1486	1506	1487, 1429	
δ(CH)het+ δ(NH)	1471, 1363, 1286	1463, 1321	1435	1393 1355	1388, 1384
ν(CN)	1577	1480, 1350[h], 1323		1310[h], 1275[g]	1316[h]
δ(CH)het	1170, 1125	1359		1245, 1134	1272, 1134
δ(CH)arom	1348, 1340, 1331, 1155	1339		1291, 1170, 1121	1291, 1172, 1117
δ(NH)	1443	–		1208[i]	1229
$\nu(SO)_{as}$	1303	1277	1350	1336	1308
$\nu(N=N)$				1186	1180
$\nu(SC) + \nu(SO)_s$	1140, 1101	1142, 1096	1330	1114, 1062	1108, 1057
ν(C–Cl)				1078	1085
$\delta(NH_2)_{as}$	1075	1084		1027	1003
ν(NS)	917	915		856	862, 759
γ(CH)het	1019	1017, 866		970, 839	954, 816
γ(CH)arom				945, 930	942, 933, 809

[a] Normal vibration modes, as=asymmetric, *s*= symmetric, arom=aromatic, het=heterocyclic, umb=umbrella.
[b] Values from experimental data [16].
[c] In alpha position with respect to the SO group.
[d] In the anti zone with respect to the N–H bond.
[e] In alpha position with respect to the amino group.
[f] For those H that are in syn with respect to the N–H bond.
[g] ν(CN) coupled with other heterocyclic ring vibrations.
[h] CNH_2.
[i] Coupled with $\nu(N=N)$ and other heterocyclic ring vibrations.

Table 7
Calculated IR frequencies (cm^{-1}) of the sulphonamides SCM.

Mode [a]	SCM_{syn}	SCM_{anti}	SCM_{exp} [b]	SCM_{synQE}	SCM_{antiQE}
$\nu(NH_2)_{as}$	3699	3704	3471	3596	3631
$\nu(NH_2)_s$	3584	3588	3381	3382	3518
ν(NH)	3526	3556	3257	3473	3509
ν(CH)arom	3213[c], 3204[d], 3202[c], 3190[d]	3218[c], 3205[d]	3232	3136, 3125 3109, 3100	3148, 3127 3105, 3100
$\nu(CH)_{as}$ CH_3	3193,3150	3199, 3147	3114	3096, 3051	3096, 3040
$\nu(CH)_s$ CH_3	3073	3072	2918	2987	2978
$\nu(C=O)$	1744	1745	1686	1664	1712
Ring arom.	1657, 1638	1655, 1639	1640	1600	1560
$\delta(NH_2)_s$	1627	1619	1596	1626	1605
δ(CH)arom	1538, 1484	1541, 1483	1505	1492, 1439	1486, 1430
$\delta(CH_3)_{as}$	1474, 1452	1474, 1457	1469	1421, 1414	1427, 1419
$\delta(CH_3)_s$		1434	1418	1362	1365
ν(CN)	1349[e]	1348[e], 1245[f]		1281	1309
$\delta(CH_3)$umb	1401	1398	1375	1349	1333
δ(CH)arom	1371, 1334, 1205, 1158	1373, 1332, 1208, 1156	1322	1332, 1290 1173, 1120	1288, 1175 1166, 1118
δ(NH)	1394	1434	1245	1272	1350
$\nu(SO)_{as}$	1294	1292	1191	1326	1298
$\nu(SC) + \nu(SO)_s$	1138, 1101	1139, 1099	1155	1114	1109
$\delta(NH_2)_{as}$	1080	1075	1091	1040	1026
$\delta(CH_3)$	1055, 1039	1064, 1022		1017, 991	1009, 945
δ(CH)arom	998, 975	994, 970	995	946, 934	944, 933
ν(NS)	948	861	857	885	774

[a] Normal vibration modes, as=asymmetric, *s*= symmetric, arom=aromatic, het=heterocyclic, umb=umbrella.
[b] Values from experimental data [17,40].
[c] In the anti zone with respect to the N–H bond.
[d] In the zone syn with respect to the N–H bond.
[e] CNH_2.
[f] Amide group.

Table 8
Calculated IR frequencies (cm^{-1}) of sulfonimide tautomers.

Mode [a]	SMT_t	$SMX_{anti\_}t$	$SMX_{syn\_}t$	$SCP_{syn\_}t$	$SCP_{anti\_}t$	$SCM_{anti\_}t$	$SCM_{syn\_}t$
$\nu(NH_2)_{as}$	3693	3683	3688	3691	3683	3691	3688
$\nu(NH_2)_s$	3584	3574	3579	3582	3575	3581	3577
ν(NH)	3454	3543	3583	3558	3537	3796[c]	3802[c]
ν(CH)arom	3212_s	3226, 3215	3202_s	3200_s[g]	3228_s[g]	3213_s	3207_s, 3201_s
ν(CH)het	3247	3293	3291	3252, 3224	3244_s, 3229_{as}		
ν(CH)arom	3210_{as},3200_{as}[f] 3196[d]	3203, 3202	3191_{as}, 3190_{as} 3210_s[d]	3184_{as}, 3196_s 3187_{as}[g]	3211_{as}[g], 3217_s 3202_{as}	3212_{as}, 3199[d] 3192[e]	3192_{as}[g], 3189
$\nu(CH)_{as}$ CH_3	3191[f], 3168[d], 3147[d], 3141[f]	3177, 3143	3180, 3142			3210, 3145	3197, 3151
$\nu(CH)_s$ CH_3	3074	3070	3068			3072	3072
Ring het	1691, 1634	1678	1666, 1464, 1366	1695, 1625	1705, 1646[i]		
Ring arom.	1665, 1642, 1560, 1366	1663, 1645, 1544	1660, 1646, 1545	1661, 1643, 1366	1658, 1642	1659, 1643, 1370	1662, 1642, 1370
$\delta(NH_2)_s$	1627	1619	1618	1622	1624	1618	1623
δ(CH)arom	1540, 1480, 1332, 1205, 1157	1481, 1338, 1333, 1212, 1161	1475, 1333, 1209, 1156	1538, 1476	1543, 1479, 1367, 1340, 1214	1537, 1478, 1327, 1200_s, 1149	1538, 1481, 1329, 1201_s, 1153
$\delta(CH)_{het}$ $+\delta$(NH)	1201	1376, 1208	1248	1442	1447		
$\delta(CH_3)_{as}$	1474, 1460[f], 1461[d]	1462, 1450, 1435	1455, 1440			1466, 1445	1510, 1449
ν(CN)	1560, 1337[f], 1273_{het}	1604[b]	1599[b], 1340[f]	1577, 1430	1585, 1456, 1342[f]	1683, 1336[f]	1680, 1340[f]
δ (CH_3)umb	1407, 1401	1399	1401[i], 1381[i]			1424	1398
δ (COH)						1268	1318
$\nu(SO)_{as}$	1218	1239	1228	1240	1242	1249	1255
ν(ON)		1156	1205, 1167				
ν(SC)	1131	1138	1141	1133	1142	1134	1135
ν(SN)	1144	870	909				
$\nu(SO)_s$	1067	1081	1090		1082	1093	1097
δ $(NH_2)_{as}$	1092	1088	1081	1083	1089	1081	1086
δ (CH_3)	1059, 1055	1065	1055			1068, 1048	1064, 1049
δ (CH)	998[j], 862, 854[j]	1014–984[j], 863[j], 817	995[j], 844[j], 805	1022, 1019, 992	1010, 978	1007, 981	992
δ (NH)	783						
δ(SNC)	696	757	762			778	987[h]

[a] Normal vibration modes, as=asymmetric, *s*= symmetric, arom= aromatic, het= heterocyclic, umb=umbrella.
[b] ν(SN–C) vibration mode.
[c] Enol OH group.
[d] In syn position with respect to the OH group.
[e] In anti position with respect to the OH group.
[f] CNH_2.
[g] Both C–H bonds coplanar to the $S = O$ bond.
[h] OCN bond angle.
[i] Coupled with δ(NH).
[j] Aromatic ring.

ferent frequencies, being significantly smaller in the sulfonimide, SMT_t, tautomer of SMT than in the sulfonamide form. On the contrary, in the conformer syn of SMX this vibration mode appears at higher frequency in the sulfonimide tautomer, $SMX_{syn\_}t$, than in the sulfonamide form. The conformer anti of SMX shows similar frequencies for both tautomers. On the contrary, the conformer anti of SMX (SMXanti_t) and SCP (SCPanti_t) show lower ν(NH) frequencies than in the syn conformer (SMXsyn_t and SCPsyn_t). In SCM there is not NH group and only the ν(OH) vibration mode appears at higher frequency than the actual ν(NH) mode. The vibration modes ν(CH) of the aromatic and heterocyclic rings, and methyl groups, and the vibration of the ring structures, and the bending δ(CH) mode show similar frequencies for both tautomers. Notice, the $\nu(SO)_{as}$ mode shows higher frequencies in the sulfonamide tautomers than in the sulfonamide forms, being consistent of the longer S = O bond lengths in the last forms due to the electron rearrangement changes. Similar effects are observed in the frequencies calculated with QE (Table S3).

5. Conclusions

Several insights of the geometrical, conformational and spectroscopical properties in these arylsulfonamides, SMT, SMX, SCP and SCM, have been shown in this work. Two main conformers can be considered in these molecules, anti and syn conformers, being more probable the syn one owing to its lower energy. Nevertheless, the energy differences between these conformers are low and both conformers can occur at room temperature.

Two kind of tautomers can be considered in these molecules: the sulfonamide-sulfonimide tautomers, and sulfonyl-thioenol tautomers. The sulfonimide tautomers are less stable than the sulfonamide ones with low energy differences. However, the TS's of the reaction path were localized finding that the activation energy for its tautomerism is quite high. On the other hand, the sulfonyl tautomers are much more probable than the thioenol ones with higher energy differences and energy barriers than in the former tautomerism.

In spite of the possible candidates for polymorphism reported for the SMT crystals, all these forms are actually only one crystal form. Our calculations of the periodical tridimensional crystal structure and XRD patterns have identified these crystal forms as only one crystal form. The main intermolecular interactions responsible of the high packing energy of this crystal are the π-π interactions between the aromatic and heterocyclic rings and the H bonds between sulfonyl and amino groups and between the NH group and the heterocyclic N atom. Further studies of crystal structures of other sulphonamides will performed in future.

Our calculations allow knowing the way of the infrared frequencies of these sulphonamides change between conformers and tautomers. Hence, this spectroscopical technique can be useful to identify these forms in experimental dissolutions and crystal structures.

Author statement

All authors have seen and approved the final version of the manuscript being submitted. This manuscript is the authors' original work, hasn't received prior publication and isn't under consideration for publication elsewhere.

Data availability statement

Data freely available on request from the authors

Declaration of Competing Interest

The authors declare that they have no known competing financial interests or personal relationships that could have appeared to influence the work reported in this paper.

Acknowledgments

The authors would like to acknowledge the contribution of the European COST Action CA17120 supported by the EU Framework Programme Horizon 2020, and thank the Computational Center of CSIC and Supercomputing Center Alhambra of UGR for the high-performance computing services, and Spanish projects FIS2016–77692-C2–2-P and PCIN-2017–098, and the Andalusian project P18-RT-3786 for financial support. A.P. de la Luz thanks to Secretaría de Educación, Ciencia, Tecnología e Innovación (SECTEI) of the Mexico City for the scholarship for the postdoctoral stay. The authors are grateful to the Dirección General de Cómputo y de Tecnologías de Información y Comunicación (DGCTIC) at the Universidad Nacional Autónoma de México (UNAM) for allocation of computer time in the supercomputer (Miztli, LANCAD-UNAM-DGTIC-203).

Supplementary materials

Supplementary material associated with this article can be found, in the online version, at doi:10.1016/j.molstruc.2021.131717.

References

[1] M.E. Wolff, Burger's Medicinal Chemistry, Part II, Wiley & Sons, New York, 1979 fourth ed..
[2] P. Sukul, M. Spiteller, Sulfonamides in the environment as veterinary drugs, Rev. Environ. Contam. Toxicol 187 (2006) 67–101, doi:10.1007/0-387-32885-8_2.
[3] M.J. Mengelers, P.E. Hougee, L.H. Janssen, A.S. Van Miert, Structure-activity relationships between antibacterial activities and physicochemical properties of sulfonamides, J. Vet. Pharmacol. Therapeut. 20 (1997) 276–283, doi:10.1046/j.1365-2885.1997.00063.x.
[4] K. Weiss, W. Schüssler, M. Porzelt, Sulfamethazine and flubendazole in seepage water after the sprinkling of manured areas, Chemosphere 72 (9) (2008) 1292–1297, doi:10.1016/j.chemosphere.2008.04.053.
[5] M.Y. Haller, S.R. Müller, C.S. McArdell, A.C. Alder, M.J.F. Suter, Quantification of veterinary antibiotics (sulfonamides and trimethoprim) in animal manure by liquid chromatography–mass spectrometry, J. Chromatogr. A. 952 (1–2) (2002) 111–120, doi:10.1016/s0021-9673(02)00083-3.
[6] S.S. Chourasiya, D.R. Patel, C.M. Nagaraja, A.K. Chakraborti, P.V. Bharatam, Sulfonamide vs. sulfonimide: tautomerism and electronic structure analysis of N-heterocyclic arenesulfonamides, New J. Chem. 41 (2017) 8118–8129, doi:10.1039/C7NJ01353A.
[7] S.S. Yang, J.K. Guillory, Polymorphism in sulfonamides, J. Pharm. Sci. 61 (1) (1972) 26–40, doi:10.1002/jps.2600610104.
[8] A. Borrego-Sánchez, C. Viseras, C. Aguzzi, C.I. Sainz-Díaz, Molecular and crystal structure of praziquantel. Spectroscopic properties and crystal polymorphism, Eur. J. Pharm. Sci. 92 (2016) 266–275, doi:10.1016/j.ejps.2016.04.023.
[9] A. Borrego-Sánchez, A. Hernández-Laguna, C.I. Sainz-Díaz, Molecular modeling and infrared and Raman spectroscopy of the crystal structure of the chiral antiparasitic drug Praziquantel, J. Mol. Model. 23 (4) (2017) 106, doi:10.1007/s00894-017-3266-3.
[10] M. Francisco-Márquez, C. Soriano-Correa, C.I. Sainz-Díaz, Adsorption of sulfonamides on phyllosilicate surfaces by molecular modeling calculations, J. Phys. Chem. C. 121 (2017) 2905–2914, doi:10.1021/acs.jpcc.6b12467.
[11] C. Soriano-Correa, C. Barrientos-Salcedo, M. Francisco-Márquez, C.I. Sainz-Díaz, Computational study of substituent effects on the acidity, toxicity and chemical reactivity of bacteriostatic sulphonamides, J. Mol. Graph. Model. 81 (2018) 116–124, doi:10.1016/j.jmgm.2018.02.006.
[12] C.I. Sainz-Díaz, M. Francisco-Márquez, C. Soriano-Correa, Polymorphism, intermolecular interactions, and spectroscopic properties in crystal structures of sulphonamides, J. Pharm. Sci. 107 (2018) 273–285, doi:10.1016/j.xphs.2017.10.015.
[13] A.K. Basak, S.K. Mazumdar, S. Chaudhuri, Structure of sulphamethazine [4-amino-N-(4,6-di-methyl-2-pyrimidinyl)benzenesulphonamide], $C_{12}H_{14}N_4O_2S$, Acta Cryst. C39 (1983) 492–494, doi:10.1107/S0108270183005247.
[14] R.K. Tiwari, M. Haridas, T.P. Singh, Structure of 4-Amino-N-(4,6-dimethyl-2-pyrimidinyl)-benzenesulfonamide, $C_{12}H_{14}N_4O_2S$. Acta Cryst. C40 (1984) 655–657, doi:10.1107/S0108270184005229.
[15] L. Maury, J. Rambaud, B. Pauvert, Y. Lasserre, G. Bergé, M. Audran, Physicochemical and structural study of sulfamethazine, J. Pharm. Sci. 74 (1985) 422–426.
[16] S. SeethaLekshmi, S. Amrutha, M.S.R.N. Kiran, S. Varughese, Structural landscape of an antimicrobial sulfa drug Sulfachloropyridazine: polymorphs, solvates, and cocrystals, Cryst. Growth Des 19 (6) (2019) 3222–3232, doi:10.1021/acs.cgd.9b00083.
[17] U.H. Patel, S.A. Gandhi, Quantum chemical studies on crystals structures of sulphacetamide and sulphasalazine, Indian J. Pure Appl. Phys. 49 (2011) 263–269.
[18] M.J. Frisch, G.W. Trucks, H.B. Schlegel, G.E. Scuseria, M.A. Robb, J.R. Cheeseman, G. Scalmani, V. Barone, B. Mennucci, G.A. Petersson, H. Nakatsuji, M. Caricato, X. Li, H.P. Hratchian, A.F. Izmaylov, J. Bloino, G. Zheng, J.L. Sonnenberg, M. Hada, M. Ehara, K. Toyota, R. Fukuda, J. Hasegawa, M. Ishida, T. Nakajima, Y. Honda, O. Kitao, H. Nakai, T. Vreven, J.A. Montgomery Jr., J.E. Peralta, F. Ogliaro, M. Bearpark, J.J. Heyd, E. Brothers, K.N. Kudin, V.N. Staroverov, R. Kobayashi, J. Normand, K. Raghavachari, A. Rendell, J.C. Burant, S.S. Iyengar, J. Tomasi, M. Cossi, N. Rega, N.J. Millam, M. Klene, J.E. Knox, J.B. Cross, V. Bakken, C. Adamo, J. Jaramillo, R. Gomperts, R.E. Stratmann, O. Yazyev, A.J. Austin, R. Cammi, C. Pomelli, J.W. Ochterski, R.L. Martin, K. Morokuma, V.G. Zakrzewski, G.A. Voth, P. Salvador, J.J. Dannenberg, S. Dapprich, A.D. Daniels, O. Farkas, J.B. Foresman, J.V. Ortiz, J. Cioslowski, D.J. Fox, Gaussian 09, Revision E.01, Gaussian Inc, Wallingford CT, 2010.
[19] Y. Zhao, D.G. Truhlar, The M06 suite of density functionals for main group thermochemistry, thermochemical kinetics, noncovalent interactions, excited states, and transition elements: two new functionals and systematic testing of four M06-class functionals and 12 other functionals, Theor. Chem. Acc. 120 (2008) 215–241, doi:10.1007/s00214-007-0310-x.
[20] S.E. Wheeler, K.N. Houk, Integration grid errors for meta-GGA-predicted reaction energies: origin of grid errors for the M06 suite of functionals, J. Chem. Theor. Comput. 6 (2010) 395–404, doi:10.1021/ct900639j.
[21] W.J. Hehre, L. Radom, P.V.R. Schleyer, J.A. People, Initio Molecular Orbital Theory, John Wiley & Sons, New York, 1986, doi:10.1002/jcc.540070314.
[22] A.V. Marenich, C.J. Cramer, D.G. Truhlar, Universal solvation model based on solute electron density and on a continuum model of the solvent defined by the bulk dielectric constant and atomic surface tensions, J. Phys. Chem. B. 113 (2009) 6378–6396, doi:10.1021/jp810292n.
[23] A. Borrego-Sánchez, M.E. Awad, C.I. Sainz-Díaz, Molecular modeling of Adsorption of 5-Aminosalicylic Acid in the Halloysite Nanotube, Minerals. 8 (2) (2018) 61, doi:10.3390/min8020061.
[24] E. Carazo, A. Borrego-Sánchez, F. García-Villén, R. Sánchez-Espejo, C. Aguzzi, C. Viseras, C.I. Sainz-Díaz, P. Cerezo, Assessment of halloysite nanotubes as vehicles of isoniazid, Colloids Surf. B Biointerfaces 160 (2017) 337–344, doi:10.1016/j.colsurfb.2017.09.036.
[25] E. Escamilla-Roa, A. Hernández-Laguna, C.I. Sainz-Díaz, Theoretical study of the hydrogen bonding and infrared spectroscopy in the cis-vacant polymorph of dioctahedral 2:1 phyllosilicates, J. Mol. Model. 20 (9) (2014) 2404, doi:10.1007/s00894-014-2404-4.
[26] E. Escamilla-Roa, F.J. Huertas, A. Hernández-Laguna, C.I. Sainz-Díaz, A DFT study of the adsorption of glycine in the interlayer space of montmorillonite, Phys. Chem. Chem. Phys. 19 (23) (2017) 14961–14971, doi:10.1039/c7cp02300f.
[27] P. Giannozzi, O. Andreussi, T. Brumme, O. Bunau, M.B. Nardelli, M. Calandra, R. Car, C. Cavazzoni, D. Ceresoli, M. Cococcioni, N. Colonna, I. Carn-

imeo, A. Dal Corso, S. de Gironcoli, P. Delugas, R.A. DiStasio Jr, A. Ferretti, A. Floris, G. Fratesi, G. Fugallo, R. Gebauer, U. Gerstmann, F. Giustino, T. Gorni, J. Jia, M. Kawamura, H.-Y. Ko, A. Kokalj, E. Küçükbenli, M. Lazzeri, M. Marsili, N. Marzari, F. Mauri, N.L. Nguyen, H.-V. Nguyen, A. Otero-de-la-Roza, L. Paulatto, S. Poncé, D. Rocca, R. Sabatini, B. Santra, M. Schlipf, A.P. Seitsonen, A. Smogunov, I. Timrov, T. Thonhauser, P. Umari, N. Vast, X. Wu, S. Baroni, Advanced capabilities for materials modelling with QUANTUM ESPRESSO, J. Phys.: Condens. Matter. 29 (46) (2017) 465901, doi:10.1088/1361-648X/aa8f79.

[28] J.P. Perdew, K. Burke, M. Ernzerhof, Generalized Gradient Approximation Made Simple, Phys. Rev. Lett. 77 (1996) 3865–3868, doi:10.1103/PhysRevLett.77.3865.

[29] P.E. Blöchl, Projector augmented-wave method, Phys. Rev. B Condens. Matter. 50 (1994) 17953–17979, doi:10.1103/physrevb.50.17953.

[30] S. Grimme, J. Antony, S. Ehrlich, H. Krieg, A consistent and accurate *ab initio* parametrization of density functional dispersion correction (DFT-D) for the 94 elements H-Pu, J. Chem. Phys. 132 (2010) 154104, doi:10.1063/1.3382344.

[31] S. Baroni, S. de Gironcoli, A. Dal Corso, P. Dal Giannozzi, Phonons and related crystal properties from density-functional perturbation theory, Rev. Mod. Phys. 73 (2) (2001) 515–562, doi:10.1103/RevModPhys.73.515.

[32] G. Schaftenaar, J.H. Noordik, Molden: a pre- and post-processing program for molecular and electronic structures, J. Comput. Aided Mol. Design. 14 (2000) 123–134, doi:10.1023/A:1008193805436.

[33] Biovia, Materials Studio, 2016, Dassault Systems.

[34] D. Das, N. Sahu, S. Roy, P. Dutta, S. Mondal, E.L. Torres, C. Sinha, The crystal structure of sulfamethoxazole, interaction with DNA, DFT calculation, and molecular docking studies, Spectrochim. Acta Part A Mol. Biomol. Spectroscopy. 137 (2015) 560–568, doi:10.1016/j.saa.2014.08.034.

[35] Z. Ettehadi, A. Davoodnia, M. Khashi, S.A. Beyramabadi, Tautomerism in the sulfonamide moiety: synthesis, experimental and theoretical characterizations, J. Struct. Chem. 59 (2018) 1596–1609, doi:10.1134/S0022476618070119.

[36] R.J. Mesley, C.A. Johnson, Infrared identification of pharmaceutically important sulphonamides with particular reference to the occurrence of polymorphism, J. Pharm. Pharmacol. 17 (1965) 329–340, doi:10.1111/j.2042-7158.1965.tb07679.x.

[37] M. Kuhnert-Brandstatter, S. Wunsch, Polymorphism and mixed crystal formation in sulfonamides and related compounds, Mikrochim. Acta. 6 (1969) 1297–1307.

[38] G. Ogruc-Ildiz, S. Akyuz, A.E. Ozel, Experimental, *ab initio* and density functional theory studies on sulfadiazine, J. Mol. Struct. 924 (2009) 514–522.

[39] C. Topacli, A. Topacli, Infrared spectra simulation for some sulphonamides by using semi-empirical methods, Spectroscopy Lett 35 (2) (2002) 207–217, doi:10.1081/SL-120003806.

[40] N.R. Goud, R.A. Khan, A. Nangia, Modulating the solubility of Sulfacetamide by means of cocrystals, Cryst. Eng. Comm. 16 (2014) 5859–5869, doi:10.1039/c4ce00103f.